Are neutrinos Dirac or Majorana particles? Experimental search for neutrinoless beta decay

Trabajo Fin de Grado (Bachelor Thesis)

Written by

Nicolás Rodríguez Galván

nicorodrigal@gmail.com

Supervised by

Manuela Rodríguez Gallardo

Joaquín José Gómez Camacho

June 2021

Contents

1 Introduction

The neutrino is a very common particle in the universe and yet very hard to detect. It was postulated by Enrico Fermi in 1930 and it is included in the Standard Model as a masless and non-charged particle. Neutrinos feel only the weak force. Lastly, they exist in three flavours: electron, muon and tau.

In the context of quantum field theory, a Dirac particle is a particle which is different from its antiparticle. In contrast, a Majorana particle is a particle which is equal to its antiparticle. According to the Standard Model, all fermions belongs to the category of Dirac particles [1]. Nevertheless, neutrinos might be an exception.

Majorana particles do not have any conserved charge-like quantum number because it would induce to distinguish between the particle and its antiparticle. This means that the particle must be neutral. The only fermion that fulfils this condition is the neutrino [2].

The goal of the first part of this work is to discuss the mathematical background of Dirac and Majorana particles. For this purpose, the Dirac and Majorana lagrangian mass terms are derived from the lagrangian of $\frac{1}{2}$-spin particles. Moreover, their properties are explained and the differences among the massless, Majorana and Dirac case or cases are discussed.

The second part consists in the search for experimental evidence that could verify the identity of neutrinos. Are they Dirac or Majorana particles? For this purpose, the double beta decay is addressed. The use of this kind of decay in experiments is the best procedure to investigate their nature.

The beta decay minus consists in the decay of a neutron into a proton with an emission of an electron and a antineutrino:

$$\mathcal{N}(A, Z) \rightarrow \mathcal{N}(A, Z + 1) + e^{-} + \bar{\nu}_e \tag{1}$$

where A and Z are the mass and atomic numbers, respectively.

The beta decay is forbidden in some even-even nuclei because energetically is not favourable (the final energy would be higher). However, these elements can decay through a double beta decay due to the fact that they decay into more tightly bounded nuclei. In this case, the

corresponding equation for the double β^- decay ($2\nu\beta\beta-$) is

$$\mathcal{N}(A, Z) \rightarrow \mathcal{N}(A, Z + 2) + 2e^- + 2\bar{\nu}_e. \tag{2}$$

Theoretically, a neutrinoless double beta decay ($0\nu\beta\beta-$) is also possible. Moreover this could be experimentally confirmed. Whereas in $2\nu\beta\beta-$decays, electron energies correspond to a broad spectrum, in $0\nu\beta\beta-$decays the two electrons would carry the total energy and a peak, instead of a spectrum, would be observed. The goal of every experiment related to neutrinoless double beta decay is to find this peculiar signal [3].

If neutrinoless beta decays were experimentally observed, neutrinos would be Majorana particles [4]. In this case, there would not be any difference between a neutrino and a antineutrino, so they could be emitted and absorbed in the same process without appearing in the final state. Thus, the study of this decay is very important because it can shed light on the question proposed in this work: are neutrinos Dirac or Majorana particles?

2 Neutrinos in Quantum Field Theory

2.1 The Lagrangian of $\frac{1}{2}$-spin particles and Dirac equation

In quantum field theory, fields describe the behaviour of particles. The Lagrangian, L, as a function of its general coordinates is replaced by the Lagrangian density, $\mathcal{L}$, which depends on the fields ϕ and its derivatives respect the spatial coordinates $\partial_i\phi$ $(i = 1, 2, 3)$ and time $\partial_0\phi$. Regarding $\frac{1}{2}$-spin particles, the associated field is the Dirac field $\psi(x)$. The variable x is referred to the four-vector $X^\mu = (t, \mathbf{x})$. The space and time evolution of fields are represented by the Lagrangian density.

The free Lagrangian density of spin-$\frac{1}{2}$ particles is presented below [1]

$$\mathcal{L} = \bar{\psi}(x)\left(i\hbar c\gamma^\mu\partial_\mu - mc^2\right)\psi(x), \tag{3}$$

where $\bar{\psi} = \psi^\dagger\gamma^0$ is the adjoint field, c is the speed of light in vacuum, $\hbar$ is the Planck's constant divided by 2π and m the rest mass. The matrices γ^μ, despite the μ index, are not four-vectors. Taking the Einstein convention, it is implied the summation over repeated indices. These γ-matrices satisfy the anticommuting relation

$$\{\gamma^\mu, \gamma^\nu\} = \gamma^\mu\gamma^\nu + \gamma^\nu\gamma^\mu = 2g^{\mu\nu} \qquad \nu, \mu = 0, 1, 2, 3 \tag{4}$$

and the condition

$$\gamma^0\gamma^{\mu\dagger}\gamma^0 = \gamma^\mu, \tag{5}$$

where $g^{\mu\nu}$ is the metric tensor ($g_{00} = 1$, $g_{ii} = -1$ and $g_{\mu\nu} = 0$ for $\mu \neq \nu$). The square of γ-matrices is calculated from (4)

$$\left(\gamma^0\right)^2 = 1, \quad \left(\gamma^i\right)^2 = -1 \quad (i = 1, 2, 3) \tag{6}$$

and equation (5) gives an additional constraint

$$\left(\gamma^0\right)^\dagger = \gamma^0, \quad \left(\gamma^i\right)^\dagger = -\gamma^i. \tag{7}$$

Thus, γ^0 is hermitian and γ^i are antihermitian. The last important property is that the γ-matrices are Lorentz invariant, this is they are invariant under Lorentz transformations.

[1] It is important to note that the simultaneous appearance of c and $\hbar$ in (3) implies the attempt to unify the quantum theory and the special relativity.

Pauli proved that all representations of γ-matrices are equivalent [4]. From now on, the Pauli-Dirac representation will be used. In this representation, these matrices have the following form:

$$\gamma^0 = \begin{pmatrix} 1 & 0 & 0 & 0 \\ 0 & 1 & 0 & 0 \\ 0 & 0 & -1 & 0 \\ 0 & 0 & 0 & -1 \end{pmatrix} \quad \text{and} \quad \gamma^k = \begin{pmatrix} 0 & \sigma_i \\ -\sigma_i & 0 \end{pmatrix}, \tag{8}$$

where σ_i are the Pauli matrices

$$\sigma_x = \begin{pmatrix} 0 & 1 \\ 1 & 0 \end{pmatrix}, \quad \sigma_y = \begin{pmatrix} 0 & -i \\ i & 0 \end{pmatrix}, \quad \sigma_z = \begin{pmatrix} 1 & 0 \\ 0 & -1 \end{pmatrix}. \tag{9}$$

The Euler-Lagrange equation determines the spacial and time evolution of the Dirac field

$$\partial_\mu \frac{\partial \mathcal{L}}{\partial \left(\partial_\mu \bar{\psi}\right)} = \frac{\partial \mathcal{L}}{\partial \bar{\psi}} \tag{10}$$

Hence, the Lagrangian density must be Lorentz invariant. Otherwise, two observers in two different rest frames would obtain different equations. This would violate the first postulate of special relativity: the laws of physics take the same form in all inertial frames of reference. The quantity $\overline{\psi}\gamma^\mu\psi$ behaves as a contravariant four-vector and ∂_μ as a covariant-four vector under a Lorentz transformation. Then, the product $\overline{\psi}\partial_\mu\gamma^\mu\psi$ is a Lorentz invariant and so does the Lorentz density [5].

Appling the Euler-Lagrange equation to (3),

$$\partial_\mu \frac{\partial \mathcal{L}}{\partial \left(\partial_\mu \bar{\psi}\right)} = 0 \tag{11}$$

$$\frac{\partial \mathcal{L}}{\partial \overline{\psi}} = \left(ci\hbar\gamma^\mu\partial_\mu - mc^2\right)\psi(x) \tag{12}$$

the Dirac equation is obtained

$$\left(\mathrm{i}\hbar\gamma^\mu\partial_\mu - mc\right)\psi = 0\ . \tag{13}$$

The Dirac equation presents Lorentz covariance [3]. This means that it preserve its form in every rest frame. Therefore (13) it is said to be written in a covariant form.

The lowest object that fulfills the anticommuting relation (4) are 4x4 matrices. Therefore, the solution of the Dirac equation must be a vector of four components called spinor. The spinor ψ and the adjoint spinor are represented below in order to ease the concept of a 4-component spinor:

$$\psi = \begin{pmatrix} \psi_1 \\ \psi_2 \\ \psi_3 \\ \psi_4 \end{pmatrix}, \qquad \bar{\psi} = \begin{pmatrix} \psi_1^* & \psi_2^* & -\psi_3^* & -\psi_4^* \end{pmatrix}. \tag{14}$$

In the free case, when the fermion is free of any interaction, the normalized solution to the Dirac equation is formed by a set of spinors presented below [6]

$$\Psi_{\mathbf{p}}^{(+)}(\mathbf{x},t) = \frac{1}{\sqrt{V}} u_{\mathbf{p}} e^{\frac{i}{\hbar}(\mathbf{p}\cdot\mathbf{x}-Et)}, \qquad \Psi_{\mathbf{p}}^{(-)}(\mathbf{x},t) = \frac{1}{\sqrt{V}} w_{\mathbf{p}} e^{-\frac{i}{\hbar}(\mathbf{p}\cdot\mathbf{x}-Et)} \tag{15}$$

$$u_{1,\mathbf{p}} = \sqrt{\frac{E+mc^2}{2mc^2}} \begin{pmatrix} 1 \\ 0 \\ \frac{p_z c}{E+mc^2} \\ \frac{(p_x+ip_y)c}{E+mc^2} \end{pmatrix}; \quad u_{2,\mathbf{p}} = \sqrt{\frac{E+mc^2}{2mc^2}} \begin{pmatrix} 0 \\ 1 \\ \frac{(p_x-ip_y)c}{E+mc^2} \\ \frac{-p_z c}{E+mc^2} \end{pmatrix}, \tag{16}$$

$$w_{1,\mathbf{p}} = \sqrt{\frac{E+mc^2}{2mc^2}} \begin{pmatrix} \frac{-p_z c}{E+mc^2} \\ \frac{(-p_x-ip_y)c}{E+mc^2} \\ 1 \\ 0 \end{pmatrix}; \quad w_{2,\mathbf{p}} = \sqrt{\frac{E+mc^2}{2mc^2}} \begin{pmatrix} \frac{(-p_x+ip_y)c}{E+mc^2} \\ \frac{p_z c}{E+mc^2} \\ 0 \\ 1 \end{pmatrix}. \tag{17}$$

The spinors $u_{\mathbf{p}}$ and $w_{\mathbf{p}}$ represent solutions of free particles with momentum $\mathbf{p}$ and positive and negative energy, $E = \pm\sqrt{m^2c^4 + p^2c^2}$, respectively. The adjoint spinors are:

$$\bar{u}_{1,\mathbf{p}} = \sqrt{\frac{E+mc^2}{2mc^2}} \begin{pmatrix} 1 & 0 & -\frac{p_z}{E+mc^2} & -\frac{(p_x-ip_y)c}{E+mc^2} \end{pmatrix}, \tag{18}$$

$$\bar{u}_{2,\mathbf{p}} = \sqrt{\frac{E+mc^2}{2mc^2}} \begin{pmatrix} 0 & 1 & -\frac{(p_x+ip_y)c}{E+mc^2} & \frac{p_z c}{E+mc^2} \end{pmatrix}, \tag{19}$$

$$\bar{w}_{1,\mathbf{p}} = \sqrt{\frac{E+mc^2}{2mc^2}} \begin{pmatrix} \frac{-p_z c}{E+mc^2} & \frac{(-p_x+ip_y)c}{E+mc^2} & 1 & 0 \end{pmatrix}, \tag{20}$$

$$\bar{w}_{2,\mathbf{p}} = \sqrt{\frac{E+mc^2}{2mc^2}} \begin{pmatrix} -\frac{(p_x+ip_y)c}{E+mc^2} & \frac{p_z c}{E+mc^2} & 0 & 1 \end{pmatrix}. \tag{21}$$

2.2 Dirac mass term

Let us begin defining the chirality matrix γ^5

$$\gamma^5 \equiv \gamma_5 \equiv i\gamma^0\gamma^1\gamma^2\gamma^3. \tag{22}$$

In the Dirac representation γ^5 has the form

$$\gamma^5_{\mathrm{D}} = \begin{pmatrix} 0 & 0 & 1 & 0 \\ 0 & 0 & 0 & 1 \\ 1 & 0 & 0 & 0 \\ 0 & 1 & 0 & 0 \end{pmatrix}. \tag{23}$$

This matrix (23) can be useful to compute the eigenvalues of the chirality matrix. These are +1 and -1 and the associated eigenfunctions are ψ_R and ψ_L, respectively:

$$\gamma^5\psi_R = +\psi_R, \tag{24}$$

$$\gamma^5\psi_L = -\psi_L. \tag{25}$$

They are denoted as right-hand field, ψ_R, and left-hand field, ψ_L. An important property is that a wavefunction can be always split as the sum of its chiral right-handed and left-handed field:

$$\psi = \psi_R + \psi_L, \tag{26}$$

where

$$\psi_R = \frac{1+\gamma^5}{2}\psi, \qquad\qquad \psi_L = \frac{1-\gamma^5}{2}\psi. \tag{27}$$

The chiral fields are two-component spinors. In order to prove this, let us define the chiral projection operators

$$\psi_R = P_R\psi; \qquad\qquad \psi_L = P_L\psi, \tag{28}$$

so

$$P_R = \frac{1+\gamma^5}{2}; \qquad\qquad P_L = \frac{1-\gamma^5}{2}. \tag{29}$$

They are hermitian, fulfill the usual projector properties and

$$P_R P_L = P_L P_R = 0, \tag{30}$$

$$P_R \gamma^0 = \gamma^0 P_L, \tag{31}$$

$$P_L \gamma^0 = \gamma^0 P_F, \tag{32}$$

$$\overline{\psi_R} = \overline{\psi} P_L, \tag{33}$$

$$\overline{\psi_L} = \overline{\psi} P_R. \tag{34}$$

As a result of (26), the Dirac Lagrangian density can be rewritten as

$$\mathcal{L} = \left(\overline{\psi_R} + \overline{\psi_L}\right) \left(i\hbar c \not{\partial} - mc^2\right) \left(\psi_R + \psi_L\right), \tag{35}$$

where we have used the Feynman-dagger notation $\not{A} = \gamma^\mu A_\mu$.

Developing the expression (35), we find that there are four vanishing terms

$$\overline{\psi_R} \not{\partial} \psi_L = \bar{\psi} P_L \not{\partial} P_L \psi = \overline{\psi} \not{\partial} P_R P_L \psi = 0, \tag{36}$$

$$\overline{\psi_L} \not{\partial} \psi_R = \bar{\psi} P_R \not{\partial} P_R \psi = \overline{\psi} \not{\partial} P_L P_R \psi = 0, \tag{37}$$

$$\overline{\psi_R} \psi_R = \bar{\psi} P_L P_R \psi = 0, \tag{38}$$

$$\overline{\psi_L} \psi_L = \bar{\psi} P_R P_L \psi = 0. \tag{39}$$

Then, the Lagrangian density depending on the chiral fields is presented below

$$\mathcal{L} = \overline{\psi_R} i\hbar c \not{\partial} \psi_R + \overline{\psi_L} i\hbar c \not{\partial} \psi_L - mc^2 (\overline{\psi_R} \psi_L + \overline{\psi_L} \psi_R). \tag{40}$$

The Dirac mass term is clearly

$$\mathcal{L}_m^D = -m_D c^2 (\overline{\psi_R} \psi_L + \overline{\psi_L} \psi_R). \tag{41}$$

From this last expression an important point can be made. The Dirac mass term implies that left and right states must exist for neutrinos in order to have a non-zero Dirac mass.

The field equations are, applying the Euler-Lagrange equation (3)

$$i\hbar \not{\partial} \psi_R = mc \psi_L, \tag{42}$$

$$i\hbar\partial\!\!\!/\psi_L = mc\psi_R. \tag{43}$$

Although the chiral fields have independent kinetic terms, their equations are coupled due to the mass. Therefore this is the role of the mass in the Dirac equation: it forces to the chiral fields ψ_R and ψ_L to depend on each other.

2.3 The two-component theory of massless neutrinos

After Dirac derived his famous equation in 1929, the German scientist Hermann Weyl tried to build a Lorentz invariant equation whose solution was a two-component wavefunction. He found that this was possible by taking $m = 0$ in equation (13) [7].

Neutrinos have shown to have a very small mass, less than a few electronvolts. This is four units of magnitude less than the rest mass of the electron. Consequently it seems reasonable to study the Dirac equation for the chiral fields (42) and (43) when $m = 0$. In this case, one gets the Weyl equations

$$i\hbar\partial\!\!\!/\psi_R = 0, \tag{44}$$

$$i\hbar\partial\!\!\!/\psi_L = 0. \tag{45}$$

The chiral fields ψ_L and ψ_R are called Weyls spinors because they are spinors with two components [3]. This can be visualizated in the following way. Let us write a four-component spinor as

$$\psi = \begin{pmatrix} \chi_R \\ \chi_L \end{pmatrix}, \tag{46}$$

where χ_L and χ_R are two-component spinors. Considering the γ^5 in the chiral representation [4]

$$\gamma^5_{\mathrm{C}} = \begin{pmatrix} -1 & 0 & 0 & 0 \\ 0 & -1 & 0 & 0 \\ 0 & 0 & 1 & 0 \\ 0 & 0 & 0 & 1 \end{pmatrix}. \tag{47}$$

Then, the chiral projection operators are

$$P_L = \begin{pmatrix} 0 & 0 & 0 & 0 \\ 0 & 0 & 0 & 0 \\ 0 & 0 & 1 & 0 \\ 0 & 0 & 0 & 1 \end{pmatrix}, \qquad P_R = \begin{pmatrix} 1 & 0 & 0 & 0 \\ 0 & 1 & 0 & 0 \\ 0 & 0 & 0 & 0 \\ 0 & 0 & 0 & 0 \end{pmatrix}. \tag{48}$$

Applying (28) the chiral fields are obtained, each with two independent components:

$$\psi_R = \begin{pmatrix} \chi_R \\ 0 \end{pmatrix}, \quad \psi_L = \begin{pmatrix} 0 \\ \chi_L \end{pmatrix}. \tag{49}$$

The neutrino now can be described through two independent two-component spinors. In fact, this independence implies that only one chiral field could be enough to represent the massless neutrino.

Let us see the relation between the chirality and the helicity in this case. The helicity is defined as the projection of the momentum onto the spin

$$h = \frac{\vec{S} \cdot \vec{p}}{s|\vec{p}|}. \tag{50}$$

The spin is defined as [4]

$$\vec{S} = \frac{1}{2}\vec{\Sigma}, \tag{51}$$

where

$$\Sigma^k = \gamma^0 \gamma^k \gamma^5. \tag{52}$$

For this purpose, let us assume that $\psi(x,p)$ is an eigenfunction of the four-momentum $P^\mu = i\hbar\partial_\mu$

$$P^\mu \psi(x,p) = p^\mu \psi(x,p), \tag{53}$$

which is also a solution of the massless Dirac equation

$$i\hbar \not{\partial} \psi(x,p) = 0. \tag{54}$$

The energy in special relativity is (under the approximation $m = 0$)

$$E^2 = m^2c^4 + p^2c^2 = p^2c^2, \tag{55}$$

$$p_0 = \frac{E}{c} = |\vec{p}|. \tag{56}$$

Then, (54) yields

$$\left(\gamma^0 |\vec{p}| - \vec{\gamma}\cdot\vec{p}\right)\psi(x,p) = 0. \tag{57}$$

Multiplying this last equation by $\gamma^5\gamma^0$ on the left

$$\gamma^5\gamma^0\vec{\gamma}\cdot\vec{p}\,\psi(x,p) = \gamma^5|\vec{p}|\,\psi(x,p). \tag{58}$$

Using the anticommutation relation

$$\{\gamma^5, \gamma^\mu\} = 0, \tag{59}$$

we obtain the following result

$$\frac{\vec{\Sigma}\cdot\vec{p}}{|\vec{p}|}\psi(x,p) = \gamma^5\psi(x,p). \tag{60}$$

Applying this to the chiral fields,

$$\frac{\vec{\Sigma}\cdot\vec{p}}{|\vec{p}|}\psi_R(x,p) = \gamma^5\psi_R(x,p) = +\psi_R(x,p), \tag{61}$$

$$\frac{\vec{\Sigma}\cdot\vec{p}}{|\vec{p}|}\psi_L(x,p) = \gamma^5\psi_L(x,p) = -\psi_L(x,p). \tag{62}$$

Hence, the relation between the helicity and the chirality is clear through (60): they coincide for eigenfunctions of the four-momentum which are also solution of the massless Dirac equation. Moreover, equations (61) and (62) show that a massless right-handed chiral field with a definite four-momentum has helicity $h = +1$ and a massless left-handed chiral field with a definite four-momentum has helicity $h = -1$.

In 1957, the helicity of neutrinos was successfully measured in the Goldhaber *et al* experiment [4]. They discovered that the neutrinos helicity is $h = -1$ and antineutrinos helicity is $h = 1$. Consequently, within the two-component massless theory neutrinos are described by left-handed chiral fields and antineutrinos by right-handed chiral fields.

It is known that neutrinos have masses due to neutrino oscillations [7]. If the neutrino mass is produced by the Dirac mass term, a right-handed field must exist. Nevertheless it has not been detected in experiments because it does not interact with the electroweak force. This kind of field is called sterile field.

2.4 Majorana mass term

The Italian physicist Ettore Majorana wondered if he could construct a mass term only using a left-handed chiral field. This way, nature would dispose of the neutrino right-handed field and would choose the most economical option. Before starting any calculation, let us define the concept of charge conjugation and its properties.

The charge conjugation is a discrete symmetry transformation. It consists in transforming a particle wavefunction by its respective antiparticle wavefunction through the charge conjugation operator $\hat{C}$. Let ψ be the spinor of a neutrino and ψ^C the charge-conjugated field, this transformation is defined as:

$$\psi(x) \xrightarrow{\mathrm{C}} \psi^{\mathrm{C}}(x) = \xi_{\mathrm{C}}\mathcal{C}\bar{\psi}^T(x) = -\xi_{\mathrm{C}}\gamma^0\mathcal{C}\psi^*(x). \tag{63}$$

The coefficient ξ_C is constrained since two charge conjugation transformations must leave ψ invariant

$$\psi \xrightarrow{\mathrm{C}} \xi_{\mathrm{C}}\mathcal{C}\bar{\psi}^T \xrightarrow{\mathrm{C}} |\xi_{\mathrm{C}}|^2 \psi, \tag{64}$$

so

$$|\xi_{\mathrm{C}}|^2 = 1. \tag{65}$$

In the Dirac representation [4]

$$\mathcal{C} = i\gamma^2\gamma^0 = i\begin{pmatrix} 0 & 0 & 0 & i \\ 0 & 0 & -i & 0 \\ 0 & i & 0 & 0 \\ -i & 0 & 0 & 0 \end{pmatrix}. \tag{66}$$

Then, the charge conjugated spinor is

$$\psi \to \psi^C = i\xi_C\gamma^2\psi^* = i\xi_C\begin{pmatrix} -\psi_4^* \\ \psi_3^* \\ \psi_2^* \\ -\psi_1^* \end{pmatrix}. \tag{67}$$

In the free case, the charge-conjugated spinors present the following form

$$u^C_{1,\mathbf{p}} = i\xi_C\sqrt{\frac{E+mc^2}{2mc^2}}\begin{pmatrix} -\frac{p_x-ip_y}{E+M} \\ \frac{p_z}{E+M} \\ 0 \\ -1 \end{pmatrix}; \quad u^C_{2,\mathbf{p}} = i\xi_C\sqrt{\frac{E+mc^2}{2mc^2}}\begin{pmatrix} -\frac{-p_z}{E+M} \\ \frac{p_x+ip_y}{E+M} \\ 1 \\ 0 \end{pmatrix}, \tag{68}$$

$$w^C_{1,\mathbf{p}} = i\xi_C\sqrt{\frac{E+mc^2}{2mc^2}}\begin{pmatrix} 0 \\ 1 \\ \frac{-p_x+ip_y}{E+M} \\ -\frac{-p_z}{E+M} \end{pmatrix}; \quad w^C_{2,\mathbf{p}} = i\xi_C\sqrt{\frac{E+mc^2}{2mc^2}}\begin{pmatrix} -1 \\ 0 \\ \frac{p_z}{E+M} \\ -\frac{-p_x-ip_y}{E+M} \end{pmatrix}. \tag{69}$$

The charge conjugation matrix fulfills the following relations

$$\mathcal{C}^\dagger = \mathcal{C}^{-1}, \tag{70}$$

$$\mathcal{C}^T = -\mathcal{C}, \tag{71}$$

$$\mathcal{C}\gamma_\mu^T\mathcal{C}^{-1} = -\gamma_\mu, \tag{72}$$

$$\mathcal{C}\gamma^{5^T}\mathcal{C}^{-1} = \gamma^5. \tag{73}$$

Now, let us have a look at the coupled equations for the chiral fields (42) and (43) presented again below

$$i\hbar\gamma^\mu\partial_\mu\psi_R = mc\psi_L, \tag{74}$$

$$i\hbar\gamma^\mu\partial_\mu\psi_L = mc\psi_R. \tag{75}$$

The goal is to be able to describe the mass term such that it depends on the left-handed chiral field. For this purpose, we are going to try to make the first equation (75) look like the second (74). Taking the hermitian conjugate of the first equation

$$(i\hbar\gamma^\mu\partial_\mu\psi_R)^\dagger = mc\psi_L^\dagger \tag{76}$$

$$-i\hbar\partial_\mu\psi_R^\dagger\gamma^{\mu\dagger} = mc\psi_L^\dagger \tag{77}$$

and multiplying on the right by γ^0 we get

$$-i\hbar\partial_\mu\psi_R^\dagger\gamma^{\mu\dagger}\gamma^0 = mc\psi_L^\dagger\gamma^0. \tag{78}$$

The γ-matrices property (5) multiplied by γ^0 on the left yields $\gamma^{\mu\dagger}\gamma^0 = \gamma^0\gamma^\mu$. Then,

$$-i\hbar\partial_\mu\overline{\psi_R}\gamma^\mu = mc\overline{\psi_L}. \tag{79}$$

Now, we want to get rid of the negative sign. In order to achieve this, the transpose is taken

$$-i\hbar\left[\partial_\mu\overline{\psi_R}\gamma^\mu\right]^T = mc\overline{\psi_L}^T \tag{80}$$

$$-i\hbar\gamma^{\mu T}\partial_\mu\overline{\psi_R}^T = mc\overline{\psi_L}^T. \tag{81}$$

Using the property (72),

$$i\hbar\gamma^{\mu}\partial_\mu\mathcal{C}\overline{\psi_R}^T = mc\mathcal{C}\overline{\psi_L}^T. \tag{82}$$

This last equation has the same form as (75) and they are identical assuming

$$\psi_R = \mathcal{C}\overline{\psi_L}^T. \tag{83}$$

This makes sense if $\mathcal{C}\overline{\psi_L}^T$ is a right handed component of ψ. Let us demostrate this considering the property of the charge conjugation matrix (73) in the form $P_L\mathcal{C} = \mathcal{C}P_L^T$

$$P_L\left(\mathcal{C}\overline{\psi_L}^T\right) = \mathcal{C}\left(\overline{\psi_L}P_L\right)^T = \mathcal{C}\left[\left(P_R\psi_L\right)^\dagger\gamma^0\right]^T = 0. \tag{84}$$

As the projection onto the left-handed chiral projection operator is zero, this means that $\mathcal{C}\overline{\psi_L}^T$ is a right-handed component. Then, substituting (83) into (75) yields

$$i\hbar\gamma^{\mu}\partial_\mu\psi_L = mc\mathcal{C}\overline{\psi_L}^T. \tag{85}$$

The goal has been achieved: (85) is the Dirac equation written only in terms of the left-handed field. It is called the Majorana equation.

From the definition of the charge conjugation operator (63), the term $\mathcal{C}\overline{\psi_L}^T$ is equal to the charge-conjugated field except for the coefficient ξ_C. This phase can be chosen arbitrarily [4], so it is set to be the unity. Then,

$$\psi_L^C = \mathcal{C}\overline{\psi_L}^T = \psi_R. \tag{86}$$

Assuming this convention, the field ψ becomes

$$\psi = \psi_L + \psi_R = \psi_L + \mathcal{C}\overline{\psi_L}^T = \psi_L + \psi_L^C. \tag{87}$$

This field is called the Majorana field and it fulfills the important Majorana condition

$$\psi^C = (\psi_L + \psi_L^C)^C = \psi_L^C + \psi_L = \psi. \tag{88}$$

The charged conjugated field is equal to the field itself. This has an astonishing consequence: a Majorana particle is its own anti-particle. Thus, only neutral fermions can be Majorana fermions like the neutrino. The other neutral fermion candidate to be a Majorana fermion is

the neutron. However, neutron and antineutron have equal and opposite magnetic moment. This requires that they must be described by Dirac theory [8].

If the neutrino is a Majorana particle, a left-handed field is sufficient to describe it. The corresponding Majorana mass term is obtained substituting ψ_R in the Dirac mass term by ψ_L^C

$$\mathcal{L}_m^M = -m_M c^2 \left(\overline{\psi_L^C} \psi_L + \overline{\psi_L} \psi_L^C \right). \tag{89}$$

To sum up, in order the mass term to depend only on the left chiral field the Majorana condition must be fulfilled. Consequently if the neutrino has a Majorana mass term there is no difference between a neutrino and a antineutrino.

2.5 Dirac and Majorana particles. Properties. Lepton number. Interaction.

Every elementary particle has at least two fundamental properties: the mass and the spin. In case of neutrinos and antineutrinos, their mass is very small and they have spin $s = \frac{1}{2}$. Experimentally, it has been confirmed the following statement. When a neutrino is created in a weak process, its spin is antiparallel to the direction of motion. In contrast, an antineutrino carries a spin parallel to the direction of motion. Then, they are characterised by the states left-handed LH and right-handed RH, respectively [8]. These states can change during the subsequent propagation. There are three kind of approaches to link the LH and RH states.

The first case is the one where the neutrino is $m = 0$, as it was assumed in the standard model until less than twenty years ago. In this case, the neutrino (antineutrino) moves at the speed of light and remains exactly LH (RH), just like at its creation. This endures until it "dies", for example generating the corresponding lepton ℓ^- (ℓ^+) in a charged current interaction [3]. The quantum field describing a masless neutrino is a two-component Weyl field: LH for neutrinos and RH for antineutrinos. The idea of the neutrino as a Weyl particle is rejected due to the fact they have mass.

Regarding the not massless case, neutrino and antineutrino no longer remain in the state in which they were "born". As they have mass, their speed is limited and less than the speed of light. A hypothetical observer moving at speed higher than a neutrino (but less than speed of light) would see the direction of motion reversed but the spin would remain the same.

Thus the helicity would be reversed and a neutrino created in a LH state would present a small RH component. Similarlly, an antineutrino initially RH would develop a small LH component. The quantum field describing this type of neutrinos is called Dirac field and has four independent components: ν (LH and RH) and $\bar{\nu}$ (LH and RH).

Concerning the case when neutrinos are described by a Majorana field, the components can be halved. The neutrino is equal to its antiparticle, the antineutrino, so their LH and RH component are identical two by two. Then there is no distinction between neutrino and antineutrino but only two possible states of the same particle-antiparticle. Then there are only two independent components.

To sum up, the masless Weyl neutrino is a two-component field. Neutrinos are LH and antineutrinos RH and they remain in these states unless they take part in a reaction. In the massive case, there are two possibilites. The first one is the Dirac case, where neutrinos and antineutrinos are described by four-component fields. In contrast, the Majorana neutrino has only two independent component because it is equal to its antiparticle. Then there are only two states of the same particle-antiparticle.

Once the relation between the neutrino and antineutrino has been discussed, the next step is to cover their family. Neutrinos are leptons and thus they have assigned a lepton number L. Leptons have $L = 1$, antileptons $L = -1$ and any non-leptonic particle $L = 0$ [5]. The lepton number is a symmetry of the Standard Model. Any reaction is possible if it conserves the lepton number. For this purpose, the total lepton number of the reactives must be equal to the total lepton number of the product. Let us see two examples, the first one

$$\bar{\nu} + p \rightarrow n + e^{+} \tag{90}$$

conserves the lepton number $\Delta L = 0$. Moreover, the charge is also conserved, so this decay can be observed. The second one

$$\bar{\nu} + n \rightarrow p + e^{-} \tag{91}$$

violates the conservation of the lepton number $\Delta L = 2$. Hence, the Standard Model predicts that it will never take place.

Lastly, let us discuss the way neutrinos interact with other particles. As neutrinos are leptons, they do not feel the strong force. Moreover, they are non-charged particles so they

do not feel the electromagnetic force either. Thus, they only feel the weak interaction.

Processes by the weak interactions are described through the exchange of the W^+ and W^- bosons. Their respective conjugated fields are $W^\nu(x)$ and $(W^\nu(x))^*$. $W^\nu(x)$ creates a boson W^- or annihilates its antiparticle W^+, meanwhile $(W^\nu(x))^*$ does the opposite. The form of the Lagrangian density for the weak interaction is the product of the bosons fields and the weak density current:

$$\mathcal{L}^w = \frac{g_w}{\sqrt{2}} \left(W^\mu(x) j_\mu^+(x) + (W^\mu(x))^* \, j_\mu^-(x) \right). \tag{92}$$

The weak current is the sum of a weak leptonic current and a hadronic weak current

$$j_\mu^\pm(x) = j_\mu^{\pm lep}(x) + j_\mu^{\pm had}(x). \tag{93}$$

The positive weak current for electrons has the following expression:

$$j_\mu^{+,el} = i \sum_j \bar{\psi}_{\nu_e}(x) \frac{1-\gamma_5}{2} \gamma_\mu \psi_e(x), \tag{94}$$

so the current is an operator that annihilates an antineutrino (or creates a neutrino) and annihilates an electron (or creates creates a positron). Concerning the negative weak current for electrons, it is:

$$j_\mu^{-,el} = i \sum_j \bar{\psi}_e(x) \frac{1-\gamma_5}{2} \gamma_\mu \psi_{\nu_e}(x). \tag{95}$$

Regarding the hadronic case, the weak force changes the flavour of the quarks. For instance, a weak process where a quark d is annihilated and a quark u is created is given by the current:

$$j_\mu^{+,had} = \cos(\theta_c) \, i \bar{\psi}_u(x) \frac{1-\gamma_5}{2} \gamma_\mu \psi_d(x) \tag{96}$$

where θ_c is the Cabibbo angle. On the other hand, if a quark u is annihilated and a quark d is created

$$j_\mu^{-,had} = \cos(\theta_c) \, i \bar{\psi}_d(x) \frac{1-\gamma_5}{2} \gamma_\mu \psi_u(x). \tag{97}$$

These expresions will be useful to describe the double beta decay on the next chapter.

3 Double beta decay

3.1 Description of double beta decay process. Relevant nuclei. Double beta decay with and without neutrinos

The beta minus decay is a process where a neutron decays into a proton, an electron and an electron antineutrino

$$(Z, N) \rightarrow (Z + 1, N - 1) + e^- + \bar{\nu}_e. \tag{98}$$

This process conserves the mass number and the charge. This decay is only possible if it is energetically favourable. Consequently, in terms of the mass defect $\Delta(Z, N)$ and neglecting the neutrino mass, the Q-value of the nuclear reaction must be positive

$$Q = \sum_i M_i c^2 - \sum_i M_f c^2 = \Delta(A, Z) - \Delta(A, Z + 1) > 0. \tag{99}$$

In the double beta minus decay, $2\nu\beta\beta^-$, two neutrons decay into two protons, two electrons and two electron antineutrinos:

$$(Z, N) \rightarrow (Z + 2, N - 2) + 2e^- + 2\bar{\nu}_e. \tag{100}$$

The corresponding Q-value is

$$Q = \Delta(A, Z) - \Delta(A, Z + 2). \tag{101}$$

Although double electron capture can also occur, we will focus only to this process throughout the entire document when we refer to the double beta decay. The mass number and the charge are also in this case conserved. This process is one of the rarest processes in nature with half-lives in the range of 10^{18}-10^{21} years. This is a very long period of time, greater than the age of the universe [7]. In 1987 it was experimentally observed for the first time in ^{82}Se [9]. Nowadays this kind of decay has been detected in several isotopes.

The double beta decay is observable in two different cases. The first occurs when the intermediate state cannot be reached because the single beta decay is forbidden ($Q < 0$). For instance, as it is illustrated in Figure 1, $^{76}_{32}$Ge cannot decay in $^{76}_{33}$Ar because it has a smaller binding energy. Nevertheless, $^{76}_{34}$Se has a larger binding energy so it is energetically favourable to decay through a double beta decay.

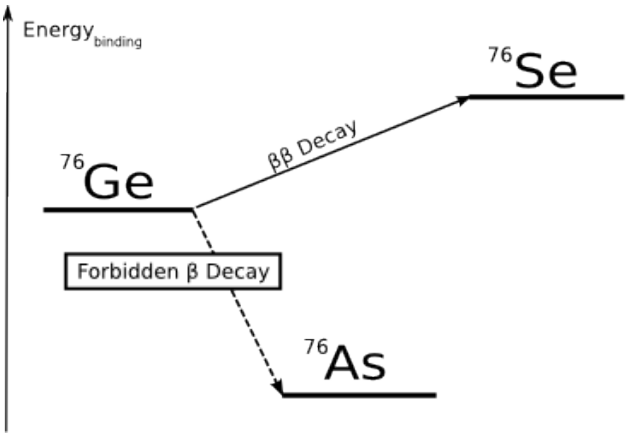

Figure 1: Decay scheme of ^{76}Ge [9].

The second possibility consists in the single beta decay being energetically allowed but the spin difference being very large. In a beta decay, the allowed transitions are those in which the difference of angular momentum is $\Delta J = 0, 1$. The forbidden decays are unlikely to occur, with $\Delta J > 1$. This is the case of $^{48}_{20}$Ca in the 0^+ state depicted in Figure 2. It can decay to $^{48}_{21}$Sc with accessible states 4^+, 5^+, 6^+. This would require either fourth- or sixth-forbidden decays [10]. An alternative possibility is to decay into $^{48}_{22}$Ti in the state 0^+. In addition to being energetically allowed, it is a $0^+ \rightarrow 0^+$ transition so it called a superallowed transition.

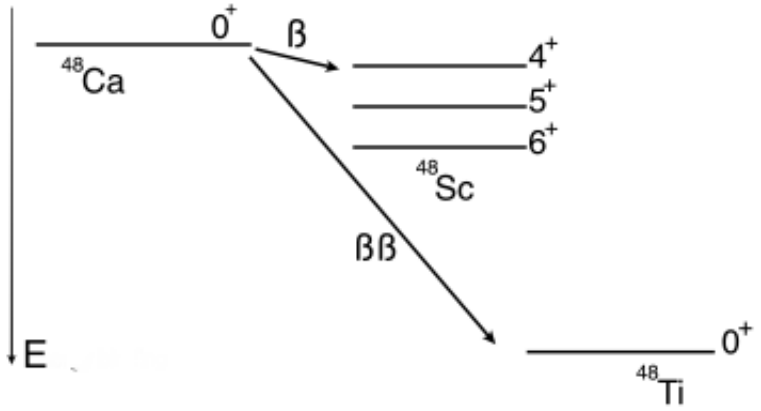

Figure 2: Decay scheme of ^{48}Ca.

The double beta decay is characterized by a long half-life and rare natural abundances [9]. Several isotopes have been proposed to undergo through double beta decay. Some nuclei which have been experimentally observed are shown in Table 1.

$2\nu\beta\beta^-$ mode	Half-life (10^{21} years) [9]
$^{48}\mathrm{Ca} \rightarrow {}^{48}\mathrm{Ti}$	0.064(13)
$^{76}\mathrm{Ge} \rightarrow {}^{76}\mathrm{Se}$	1.92(9)
$^{82}\mathrm{Se} \rightarrow {}^{82}\mathrm{Kr}$	0.096(10)
$^{96}\mathrm{Zr} \rightarrow {}^{96}\mathrm{Mo}$	0.023(3)
$^{100}\mathrm{Mo} \rightarrow {}^{100}\mathrm{Ru}$	0.00693(4)
$^{116}\mathrm{Cd} \rightarrow {}^{116}\mathrm{Sn}$	0.026(9)
$^{130}\mathrm{Te} \rightarrow {}^{130}\mathrm{Xe}$	0.82(6)
$^{136}\mathrm{Xe} \rightarrow {}^{136}\mathrm{Ba}$	2.16(8)
$^{150}\mathrm{Nd} \rightarrow {}^{150}\mathrm{Sm}$	0.10(4)

Table 1: Experimentally confirmed isotopes that undergo two-neutrino double beta decay.

In order to gain a deeper insight of the double beta decay, let us describe the force responsible of the beta decay: the weak interaction. Nucleons, like the proton and the neutron, are made up of up quarks and down quarks. The weak force changes the flavour of a quark emitting a W^- or a W^+ boson, which decays to an electron-antineutrino or a positron-neutrino pair, respectively. This can be seen in the weak currents from section 2.5. A neutron is composed of an up quark and two down quarks whereas the proton is made up of two up quarks and a down quark. In a single beta decay minus, one down quark of the neutron changes its flavour to an up quark and a W^- boson is emitted. Thus, the neutron turn into a proton and the W^- boson decays to an electron and an antineutrino.

In Figure 3a, the Feynman diagram for the double beta decay is shown. Two protons decay simultaneously into two neutrons by emitting two W^- bosons that lead to the creation of two electrons and two antineutrinos.

So far, we have only discussed the double decay in the presence of neutrinos. But is it possible to occur without them? The answer is affirmative only if neutrinos are Majorana particles. This means, as we stated before, there is no distinction between the neutrino and

the antineutrino. This kind of decay is called neutrinoless double beta decay, $0\nu\beta\beta^-$. In this case, it is assumed that first a virtual right-handed antineutrino is emitted. Then a left-handed neutrino is absorbed.

$$n \to p + e^- + \bar{\nu}, \tag{102}$$

$$\nu + n \to p + e^-. \tag{103}$$

Hence the net result is

$$2n \to 2p + 2e^-. \tag{104}$$

This can occur if the emitted right-handed antineutrino develops a left-handed component while it propagates to the second interaction. Thus any neutrino that undergo through $0\nu\beta\beta^-$ cannot be massless. In addition, the neutrino must be equal to the antineutrino. The difference respect the $2\nu\beta\beta^-$ case is that Majorana particles can be emitted and absorbed in the same process without showing up in the final state [12]. Therefore, only two electrons would be experimentally observed. The Feynman diagram for this process is depicted in Figure 3b.

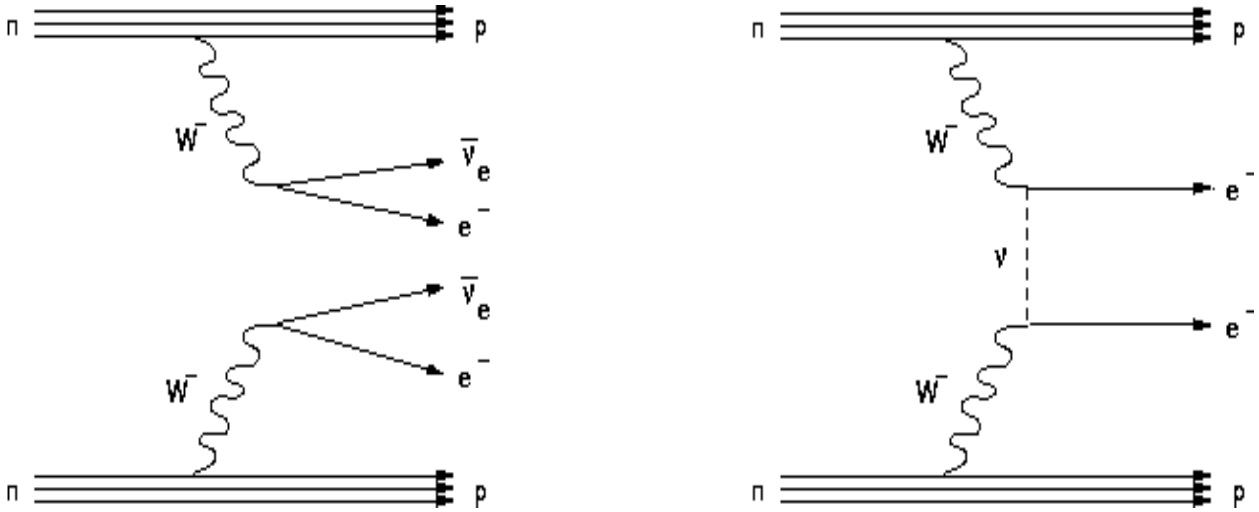

(a) Two-neutrino double beta decay.

(b) Neutrinoless double beta decay.

Figure 3: Two possibilities of double beta decay [11].

Summarising, the neutrinoless double beta decay is described by the following nuclear

reaction:

$$(Z, N) \rightarrow (Z + 2, N - 2) + 2e^{-}. \tag{105}$$

At first there is not any lepton but after the decay there are two electrons. Then the lepton number is violated by two units. The observation of $0\nu\beta\beta^{-}$ would imply three important consequences:

- Neutrinos are Majorana particles.
- Neutrinos are massive, so an indirect measurement of the neutrino mass can be made.
- The lepton number, a classical symmetry of the Standard Model, is violated.

3.2 Half-life of double beta decay. Dependence on the nuclear structure. Dependence on the neutrino mass.

An estimation of how big can be the half-life for the double beta decay can be made with the Q-value. The Fermi's golden rule states

$$W_{i \rightarrow f} = \frac{2\pi}{\hbar} \left| \langle f \left| H' \right| i \rangle \right|^2 \rho \left(E_f \right), \tag{106}$$

where $W_{i \rightarrow f}$ is the probability per unit time for the transition to occur, $|\langle f \left| H' \right| i \rangle|$ is the matrix element of the perturbation H' and $\rho(E_f)$ the density of states. The inverse of $W_{i \rightarrow f}$ is the mean life, τ. This is defined as the time in which a nuclei population is reduced by a factor of e. In contrast, the half-life is the time required to reduce the sample by a factor of 2. Thus, these quantities are proportional $T_{1/2} = \tau \ln 2$. On the other hand, the density of states is proportional to the Q-value [5]. Hence, through the Fermi's golden rule $T_{1/2}$ is inversely proportional to Q.

In order to check this proportionality, the Q-values of the decays from Table 1 have been calculated with equation (101) and with values provided by [14]. Then, the plot of the half-life in logarithm scale versus Q can be seen in Figure 4. The plot verifies our proposition: the Q-value and the half-life for double beta decay with neutrinos are inversely proportional. The greater the half-life, the smaller is the Q-value. Different nuclei have different matrix element and consequently there are fluctuations over the general tendency.

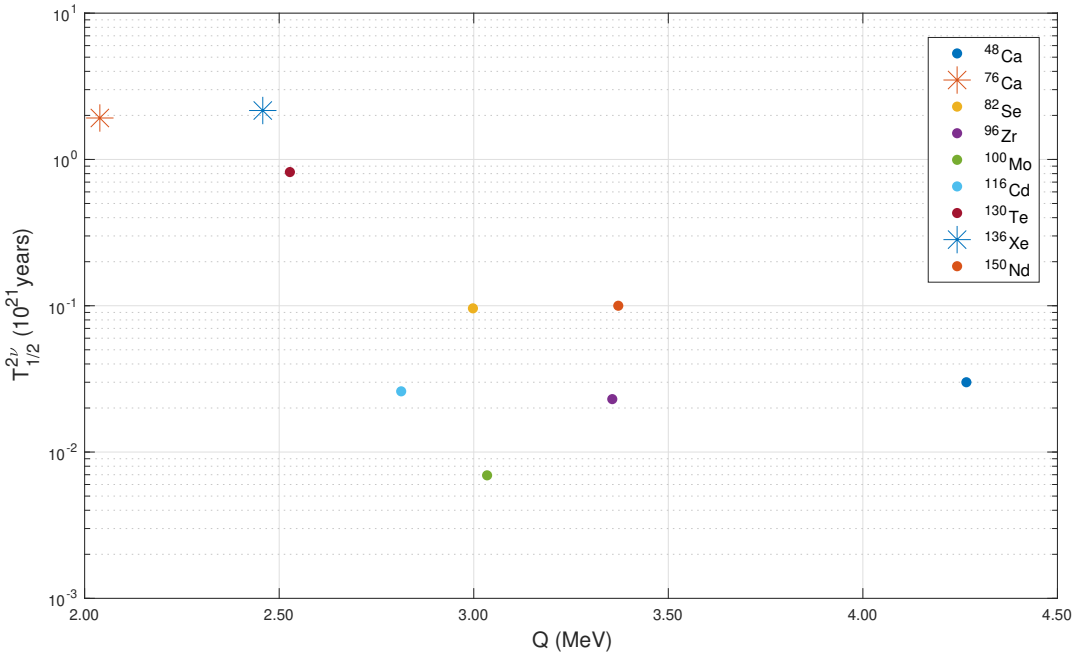

Figure 4: Half-life versus the Q-value of different $2\nu\beta\beta$ decays.

Regarding the half-life of the $0\nu\beta\beta$ decay, it is larger than the half-life for the $2\nu\beta\beta$ decay. Mathematically, the half-life for the neutrinoless decay, $T^{0\nu}_{1/2}(A, Z)$, can be summarised to depend on three terms. It has the following form [7]:

$$\frac{1}{T^{0\nu}_{1/2}(A, Z)} = \left|M^{0\nu}(A, Z)\right|^2 G^{0\nu}(Q_{\beta\beta}, Z) \left|m_{\beta\beta}\right|^2 . \tag{107}$$

The first parameter is the nuclear matrix element $|M^{0\nu}(A, Z)|$. It depends only on the nuclear structure and it is a complicated many-body nuclear problem. In order to calculate it different approximations are used. The interval of the theoretical calculated values of $|M^{0\nu}(A, Z)|$ are gathered in Table 2.

The second term $G^{0\nu}(Q_{\beta\beta}, Z)$ is a known phase space factor [13]. It depends on $Q_{\beta\beta}$, which is the Q-value of the double beta decay, and the atomic number Z. It takes into account the Coulomb interaction between electrons and the daughter nucleus.

$\beta\beta^-$ mode	$\lvert M^{0\nu}\rvert$
$^{76}\mathrm{Ge} \rightarrow {}^{76}\mathrm{Se}$	$3.59 - 10.39$
$^{100}\mathrm{Mo} \rightarrow {}^{100}\mathrm{Ru}$	$4.39 - 12.13$
$^{130}\mathrm{Te} \rightarrow {}^{130}\mathrm{Xe}$	$2.06 - 8.00$
$^{136}\mathrm{Xe} \rightarrow {}^{136}\mathrm{Ba}$	$1.85 - 6.38$

Table 2: Ranges of calculated values of $|M^{0\nu}(A,Z)|$ for several $\beta\beta^-$ modes [7].

The last parameter $|m_{\beta\beta}|^2$ is called the effective Majorana mass. It is defined as

$$m_{\beta\beta} = \sum_{k=1}^{3} U_{ek}^2 m_k, \tag{108}$$

where m_k are the mass eigenstates and U_{ek} are the matrix elements of the mixing neutrino matrix, also known as PMNS (Pontecorvo–Maki–Nakagawa–Sakata) matrix [3]. Each flavour neutrino is in a superposition of three mass eigenstates. The PMNS relates two orthonormal basis: the flavour eigenstates basis (ν_e, ν_μ, ν_τ) and the mass eigenstates basis (ν_1, ν_2, ν_3)

$$\begin{pmatrix} \nu_\mathrm{e} \\ \nu_\mu \\ \nu_\tau \end{pmatrix} = \begin{pmatrix} U_\mathrm{e1} & U_\mathrm{e2} & U_\mathrm{e3} \\ U_{\mu 1} & U_{\mu 2} & U_{\mu 3} \\ U_{\tau 1} & U_{\tau 2} & U_{\tau 3} \end{pmatrix} \begin{pmatrix} \nu_1 \\ \nu_2 \\ \nu_3 \end{pmatrix}. \tag{109}$$

These matrix elements of the PMNS matrix are experimentally known. If $T_{1/2}^{0\nu}$ is successfully measured in an experiment and $|M^{0\nu}(A,Z)|$ as well as $G^{0\nu}(Q,Z)$ are known, the effective Majorana mass can be calculated. Then the mass of neutrinos can be indirectly obtained!

3.3 Experimental set-ups for neutrinoless double beta decay

The $0\nu\beta\beta$ decay is a very rare event so it requires a big effort to be able to detect it. The main measurements obtained in this kind of experiments are the number of particles detected and their respective energy. In the double beta decay, the sum energy of the two electrons consists in a continuous spectrum. However, in the case of neutrinoless double beta decay, the energy available for electrons is only the Q-value of the decay. Then, the experimental evidence of this neutrinoless decay is a spike at the Q-value. Hence, experiments must have

good energy resolution and prevent to count background events which have similar energies to the Q-value.

The goal of neutrinoless double beta decay detection experiments is to obtain the half-life of this process. A key concept in these experiments is the sensitivity. It is defined as the the process half-life that generates a number of events which is equal to the expected background fluctuation at 1σ (68.27% confidence level, CL) [7]. To put it in another way, a $0\nu\beta\beta$ signal can be hidden in the 1σ background fluctuation if the half-life is greater than the sensitivity. An experiment that presents a larger sensitivity, have a larger half-life and consequently a smaller effective Majorana mass $m_{\beta\beta}$ according to equation (107). The experimental sensitivity of the half-life is an exclusion limit and it scales as [13]

$$T_{1/2}^{0\nu} \propto a\ \varepsilon \sqrt{\frac{M\ t}{B\ \Delta E}}, \tag{110}$$

where a is the abundance of the isotope in the source, ε is the detection efficiency for the decay process, M the total mass of the source, t the lifetime of the measurement, B the number of background counts in the relevant energy region and ΔE the energy resolution (full width at half maximum, FWHM).

Equation (107) as well as (110) depend on several isotope parameters, so different techniques can be exploited to find an experimental evidence of the $0\nu\beta\beta$ decay. The sensitivity is linear in a but this is limited because $a \leq 1$. The same holds for the efficiency. The unlimited parameters are unfortunately under a square root. This means that in order to gain an improvement of the sensitivity by a factor of two, the mass source (for instance) must increase by a factor of four.

This work focuses on two kind of experiments to detect $0\nu\beta\beta$ decay: germanium- and xenon-based detection systems.

3.3.1 Ge-based detection systems

The double beta decay of Ge^{76} is

$$^{76}\mathrm{Ge} \rightarrow {}^{76}\mathrm{Se} + 2\mathrm{e}^{-}\,(+2\bar{\nu}_{\mathrm{e}})\,. \tag{111}$$

Considering the defect masses $\Delta(^{76}\mathrm{Ge}) = -73.21288899$ MeV and $\Delta(^{76}\mathrm{Se}) = -75.25195$ MeV provided by [14], the Q-value can be calculated with (101) and it is $Q_{\beta\beta} = 2039.06$ keV.

The germanium is used as a source as well as a detector. This element is a semiconductor, so this feature is going to be exploited. The electrons produced by the $0\nu\beta\beta$ decay in the germanium interact with the lattice. The result of this interaction is the promotion of electrons to the conduction band. Thus, electron-hole pairs are formed. The energy of the emitted electrons is proportional to the number of electron-hole pairs. An external electric field is applied so it drifts the electrons and holes to the electrodes. Then a pulse is created and it can be measured through an electrical circuit. This pulse carries the information of the initial energy of the electrons produced in the decay.

The obtained measure is a voltage pulse that, after calibrating the detector, gives the sum energy of the electrons. Thus, if a $0\nu\beta\beta$ decay has been produced, the measured energy would be the Q-value.

The main advantage of this kind of detector is its high energy resolution. On the other hand, it must be cooled down. This increase the technology of the detector and the cost. In a semiconductor, electron-pairs are formed due to thermal excitation. This implies a big noise and it ruins the high energy resolution. To avoid this, the detector is cooled down to temperatures of liquid nitrogen (77.2 K). At this temperature the thermal excitation of valence electrons is highly decreased. Therefore only an energetic event such as electrons from the double beta decay can provide enough energy to promote electrons from the valence to the conduction band. The germanium systems are kept inside of a cryostat, which keeps the needed low temperature.

Moreover, the background radiation is a problem because it might have enough energy to excite electrons. Examples of the radiation to be aware are primordial radionuclides (^{238}U, ^{232}Th, ^{40}K) in the detector materials, muons from cosmic rays or radon in air. As a consequence, different kind of shields surround the cryostat to prevent noise in the measurements. Furthermore, the $2\nu\beta\beta$ decay of the germanium is an irreducible background noise. This demands a very high energy resolution.

An example of application of this detector is found in the GERDA experiment (Germanium Detector Array). It is performed at the Laboratori Nazionali del Gran Sasso in Italy. An array of high-purity germanium detectors, HPGe, are used. Eight of them are enriched up to 86% in ^{76}Ge and three are made from natural germanium. The experimental set-up is

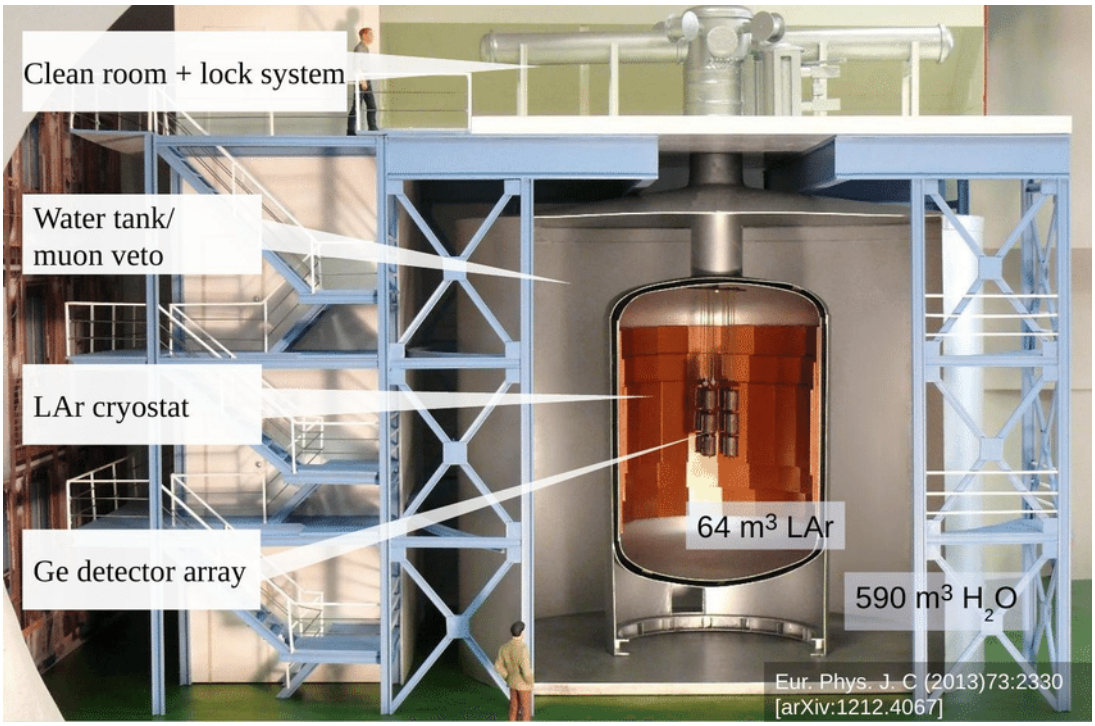

Figure 5: Experimental set-up of GERDA experiment [15].

depicted in Figure 5. The array of detectors are placed in the core, surrounded by liquid argon (LAr). This material has a double goal: act as a coolant and shield against the background radiation. All this is contained in a vacuum insulated cryostat with a volume of 64 m^3. In turn, the LAr cryostat is surrounded of 590 m^3 of pure water. The water is used as a moderator to absorb neutrons. Also, inside the water container there are 66 photomultipliers in order to detect the Cherenkov light produced by cosmic muons and hence veto the event.

3.3.2 Xe-based detection systems

The ^{136}Xe undergo under double beta decay

$$^{136}\mathrm{Xe} \rightarrow {}^{136}\mathrm{Ba} + 2\mathrm{e}^{-} \, (+2\bar{\nu}_{\mathrm{e}}) \, . \tag{112}$$

The defect mass of the nuclei are $\Delta(^{136}\mathrm{Xe}) = -86.429159$ MeV and $\Delta(^{136}\mathrm{Ba}) = -88.886921$ MeV, so the Q-value is $Q_{\beta\beta} = 2457.762$ keV.

Xenon-based detection systems are time projector chambers abbreviated as TPC. This device detects and identifies particles by reconstructing their path as they go through a volume filled with a fluid. Two kind of TPCs are used in experiments related to double beta decay: liquid xenon TPCs (LXe-TPCs) and high-pressure xenon gas TPCs (GXe-TPCs). Moreover, Xe-TPCs are also used in experiments regarding dark matter [16].

Concerning the working principle of a TPC, it consists of a charged ionizing particle that enters in the TPC and ionizes the fluid. The released electrons are drifted by an external homogeneous electric field to sensitive image planes. Then their (X,Y) position is recorded. In addition, their average drift velocity is used to convert their arrival times (relative to the event's start time) to longitudinal positions, Z.

The electric field inside the TPC is created by a cathode connected to a negative high voltage. The anode is placed on the opposite side and it is formed by anode wire planes. These planes collect the electrons and read out voltage signals. Between the cathode and the anode there is a field cage, which keeps constant the electric field. This is essential to guarantee a constant drift velocity. Considering an uniform velocity and having the electrons arrival time, is it possible to determine with good resolution the location, in the drift direction, where the ionization took place [17].

In order to determine the electron drift time, light-collection systems, such as photomultiplier tubes (PTM) and silicon photomultipliers, are used. They collect the scincillation light produced after the ionasing particle travels through the detector and set a trigger time t_0. Then, the electron drift time can be computed as the difference between the electron arrival time and the trigger time. Hence the three-dimensional reconstruction of the event can be obtained.

The energy of the decay is relatively low ($Q_{\beta\beta} = 2457.762$ keV) compared to other ionizing particles analysed in TPCs. Therefore the tracks left by the two electrons can be rather short for GXe-TPCs or even point-like objects for LXe-TPCs [16].

An example of a experiment using a Xe-based detection system is EXO-200 (Enriched Xenon Observatory). This experiment performed in United States used a LXe-TPC with 200 kg of xenon, which 80% was enriched ^{136}Xe. Another experiment that used a xenon detector is PandaX-II. It took place at China Jinping Underground Laboratory and it consisted of

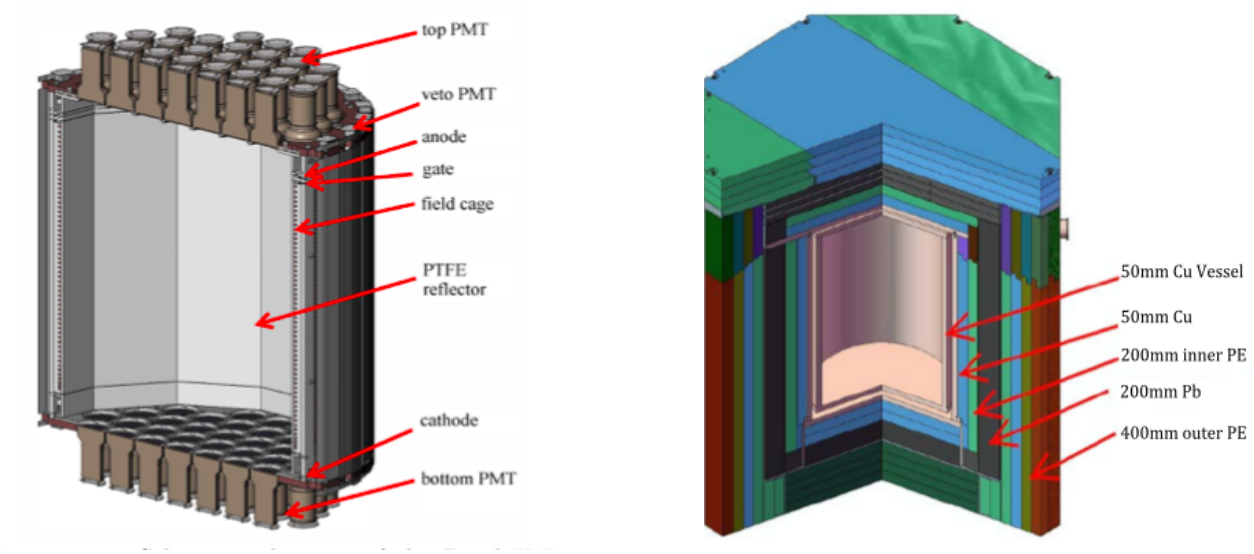

(a) TPC main components: anode, cathode, the PMTs and the field cage [18].

(b) Layered passive system shield of the detector [18].

Figure 6: PandaX-II detector schematic picture.

a dual phase xenon TPC. This kind of detector combined two phases of xenon: liquid and small portion of gas on top, so its working principle is more advanced than the usual TPC explained before.

In a dual-phase time projection chamber, photomultipliers receive two signal (whereas in GXe- and LXe-TPC PTM only get one). The main part is the liquid phase where ionization and prompt scintillation occurs. The photomultipliers receive the signal from the scintillation event and it is marked as S1. Freed electrons are drifted to the top of the liquid phase by the external electric field. In this part the drift velocity is kept constant. Then, the ionized electrons are extracted into the gas phase by a stronger field. In the gas phase, electrons produce electroluminescence and the PTMs receive the second signal S2. The difference between S2 and S1 yields the depth of the interaction.

An schematic drawing of the PandaX-II detector can be seen in Figure 6a. The vessel of dual phase TPC is cylindrical and it is made of polytetrafluoroethylene (PTFE) reflectors with a diameter of 646 mm [18]. Two sets of PTMs are placed at the top and at the bottom of

$\beta\beta^-$ mode	Experiment	$T^{0\nu}_{1/2}$ (yr)	$m_{\beta\beta}$ (eV)
^{76}Ge $\rightarrow ^{76}$Se	Heidelberg-Moscow [22]	$\geq 2.23 \cdot 10^{25}$	≤ 0.32
	GERDA [21]	$> 1.8 \cdot 10^{26}$	$< 0.079 - 0.180$
^{100}Mo $\rightarrow$ ^{100}Ru	NEMO-3 [19]	$> 2.1 \cdot 10^{23}$	$< 0.32 - 0.88$
^{130}Te $\rightarrow ^{130}$Xe	CUORICINO [20]	$> 2.8 \cdot 10^{24}$	$< 0.32 - 1.2$
^{136}Xe $\rightarrow ^{136}$Ba	PandaX-II [18]	$> 2.4 \cdot 10^{23}$	$< 1.3 - 3.5$
	EXO-200 [16]	$> 3.7 \cdot 10^{25}$	$< 0.147 - 0.398$

Table 3: Recompilation of experimental lower limits of $T^{0\nu}_{1/2}$ values at 90% confidence level and the corresponding upper limits for $m_{\beta\beta}$. About the equal sign in the Heidelberg-Moscow experiment, see the discussion below.

the chamber. In order to prevent environmental background event, the PFTE reflectors are surrounded by different layers of diverse materials like polyethylene, lead and copper. This is depicted in Figure 6b. Moreover, to prevent the radon concentration, the gap between the TPC and the innermost layer is filled with nitrogen gas [18].

Xenon is the ideal element to be used in the TPC for different reasons. First, it is a noble gas so it has a vanishing electronegativity. For this reason, released electrons do not recombine with ions and are drifted to the anode. Furthermore, xenon scintillates when energetic particles passes by. Lastly, xenon is abundant and the process of enrichment (by centrifugation) to get ^{136}Xe is very cheap and has a high production capacity. This features makes Xe-TPC to be easily scalable.

3.4 Present limits on the Majorana mass

Several experiments have been proposed and performed all over the world to find an evidence of the $0\nu\beta\beta$ decay. The results of these experiments are gathered in Table 3. Every experiment coincides in the order of magnitude of the limit on the effective Majorana mass: between 10^{-1} and 1 eV. The lowest limit is provided by GERDA in which $m_{\beta\beta} < (0.067 - 0.180)$ eV. After GERDA, the next large enriched germanium experiment carried out by LEGEND-200, will try to increase the sensitivity of the half-life up to 20^{28} years and beyond [21].

In Spain, the NEXT collaboration is building a high pressurised xenon TPC. They are

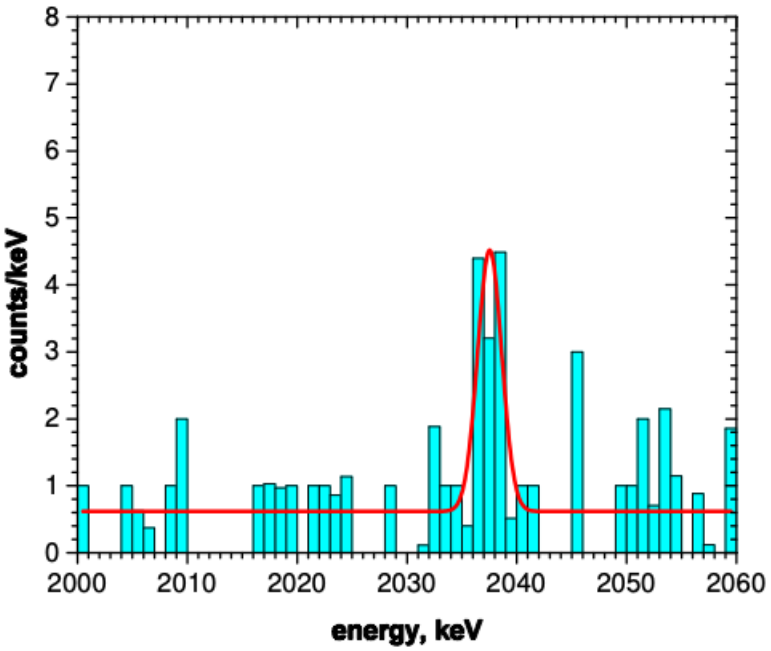

Figure 7: Sum of the spectrum of the ^{76}Ge detectors of HdM experiment. A peak is observed at $Q_{\beta\beta}$ [21].

trying to have a very good energy resolution ($< 1\%$), low background radiation and a large target mass.

Nowadays, only the Heildelberg-Moscow (HdM) experiment has claimed to have observed the $0\nu\beta\beta$ decay. They used five enriched ^{76}Ge detectors of in total 11 kg. H.V. Klapdor-Kleingrothaus (the spokeperson of the HdB experiment) alongside his colleague I. V. Krivosheina stated, after years of analysing the data, that a peak was found at $Q_{\beta\beta}$ at a significance of 6.2 σ [22]. The peak almost did not have background from any surrounding γ-rays and it is seen in Figure 7. If this is true, they claim $m_{\beta\beta} = (0.32 \pm 0.03)$ eV [22].

The HdM results are very controversial among particle physicists, due to the fact that no experiment has shown the same results. In fact, GERDA used eight detectors equal to the HdM detectors [13] and was very careful about the background, taking special care of statistical analysis techniques. In particular, one used technique was PSD (Pulse Shape Discrimination) which allows to distinguish between $0\nu\beta\beta$ like signals and photons like multi-site events. The

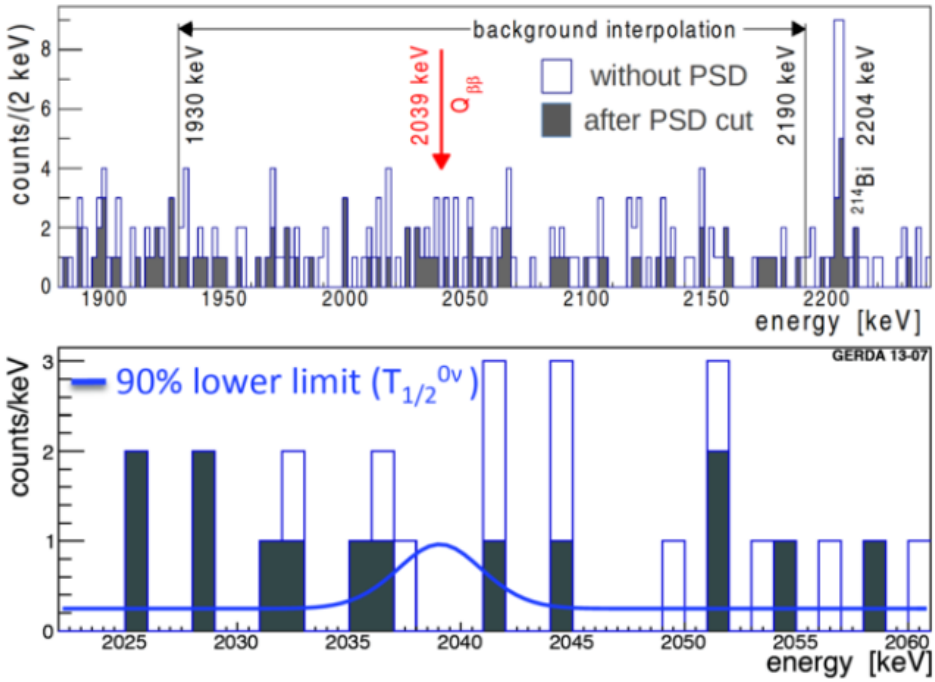

Figure 8: The combined energy spectrum from all GERDA detectors is represented. Open histogram includes PSD and filled histogram does not. The $Q_{\beta\beta}$ zone is highlighted in red without any observable peak. The upper histogram shows the region used in the background interpolation [13].

results of GERDA are presented in Figure 8. The $0\nu\beta\beta$ decay is not observed as there is not a visible peak at 2039 keV. Hence, as it used the same kind of detectors, it does not corroborate the HdM results and $0\nu\beta\beta$ decay remains to be observed.

4 Summary and conclusions

From the lagrangian for $\frac{1}{2}$-spin particles, first the Dirac mass term was obtained. The Dirac mass term forces to the neutrino to have a right-handed component which does not interact with matter (sterile). If the neutrino is a Dirac particle, there is distinction between a neutrino and a antineutrino. Then, a neutrino with a RH component and a antineutrino with a LH should exist. So far this has not been observed.

If the neutrino is a Majorana particle, the neutrino is identical to the antineutrino. There are only two possible states of the same particle-antiparticle, this is the LH and RH components of the neutrino and antineutrino are equal two by two. This Majorana idea can be verified if a neutrinoless beta decay is ever observed. Then, the lepton number would be violated by 2 units. Therefore the importance of this experiment if it is ever observed: it sheds light on the neutrino's identity and breaks the conservation of the lepton number, a fundamental symmetry of the Standard Model.

We have seen that neutrinos have a very small mass compared to other particles. The mystery of the origin of the neutrino mass has several hypothesis but it is not still solved. There are several models beyond the Standard Model that try to give an explanation of this with different lagrangian mass terms. For instance, the *see-saw mechanism* considers the neutrino to be a Majorana particle and includes in the lagrangian the Dirac mass, the Majorana mass and a general mass. It explains why the neutrino mass is much smaller than other leptons masses [7].

Concerning the double beta decay, the decay with antineutrinos have been experimentally observed with half-lives in the range of $10^{18} - 10^{21}$ years. The neutrinoless case remains unobserved with upper limits of the order of 10^{25} years. Two kind of experiments have been reviewed, each one with advantages and drawbacks. The Ge-based detector increases its sensitivity by maximizing the source mass and presents very good energy resolution. However they struggle to prevent background count events. On the other hand, the Xe-based detector system presents a lower energy resolution but they stand out for a extremely good background rejection. Furthermore, TPCs are easily scalable, a very attractive advantage.

Next experiments will try to increase the upper limit of the half-life up to 20^{28} years. Only the Heidelberg-Moscow has claimed a measurement of a $0\nu\beta\beta$ decay. However, this should be

treated with scepticism as the GERDA collaboration did not back up their results. Hence, the answer to the question proposed in this work (are neutrinos Dirac or Majorana particles?) is still unsolved.

References

[1] M. Shifman (1999). *ITEP Lectures on Particle Physics and Field Theory.*

[2] S. Esposito (2014). *The Physics of Ettore Majorana. Theoretical, Mathematical, and Phenomenological.* Cambridge University Press.

[3] M. Thomson (2013). *Modern Particle Physics.* Cambridge University Press.

[4] C. Giunti.; W. Kim, C. (2007). *Fundamentals of Neutrino Physics and Astrophysics.* Oxford University Press.

[5] J.J. Gómez Camacho (2019). *Particle physics in three credits.* University of Seville.

[6] W. Greiner; D. A. Bromley (2000). *Relativistic Quantum Mechanics.* Springer.

[7] S.M. Bilenky (2015). *Neutrino in Standard Model and beyond.* Physics of Particles and Nuclei, 46(2).

[8] F. Vissani (2015). *La domanda di Majorana.* Ithaca: Viaggio nella Scienza, 2015(6), 47-58.

[9] *Double beta decay.* Wikipedia. Retrieved on 29/04/2021.
`https://en.wikipedia.org/wiki/Double_beta_decay`

[10] S. Krane Kenneth (1998). *Introductory nuclear physics.* John Wiley & Sons.

[11] The NEMO experiment. Retrieved on 29/04/2021.
`http://nemo.in2p3.fr/physics/dbd.php`

[12] W. Rodejohann (2 May 2012). *Neutrino-less double beta decay and particle physics.* International Journal of Modern Physics E. 20(9).

[13] M. Agostini *et al.* (2016). *Search of Neutrinoless Double Beta Decay with the GERDA Experiment.* Nuclear and Particle Physics Proceedings, 273–275.

[14] Nuclear Wallet Card. Retrieved on 20/05/2021.
`https://www.nndc.bnl.gov/wallet/nwccurrent.html`

[15] V. D' Andrea (2013). *Status Report of the GERDA Phase II Startup.* Eur. Phys. J. C.

[16] M. Sorel (2019). *Xenon TPCs for Double Beta Decay Searches.* https://arxiv.org/abs/1904.06349

[17] R. Acciarri *et al.* (2015). *Summary of the Second Workshop on Liquid Argon Time Projection Chamber Research and Development in the United States.* Journal of Instrumentation, 10(11).

[18] Kaixiang Ni *et al.* (2019). *Searching for neutrino-less double beta decay of 136Xe with PandaX-II liquid xenon detector.* Chinese Physics C, 43(11).

[19] NEMO-3 Collaboration (R. Arnold *et al.*) (2014). *Search for Neutrinoless Double-Beta Decay of ^{100}Mo with the NEMO-3 Detector.* Phys. Rev. 89.

[20] CUORICINO Collaboration (E. Andreotti *et al.*) (2011). *130Te Neutrinoless Double-Beta Decay with CUORICINO.* Astropart. Phys. 34.

[21] M. Agostini *et al.* (GERDA Collaboration) (2020) *Final Results of GERDA on the Search for Neutrinoless Double-β Decay.* Phys. Rev. Lett. 125.

[22] H. V. Klapdor-Kleingrothaus and and I. V. Krivosheina (2006). *The evidence for the observation of $0\nu\beta\beta$ decay: the identification of $0\nu\beta\beta$ events from the full spectra.* Modern Physics Letters A, 21(20).